RSC Advances

PAPER

View Article Online
View Journal | View Issue

Cite this: *RSC Adv.*, 2025, **15**, 43774

UHPLC-ESI-QTOF-MS/MS profiling of saponins and tyrosinase inhibitory activity of *Ilex cochinchinensis*, *Ilex annamensis*, and *Ilex rotunda* leaves from Vietnam

Pham Hong Ngoc,[ab] Tran Chieu An,[b] Luong Van Dung,[c] Le Tien Dung[b] and Phung Van Trung*[b]

Received 16th July 2025
Accepted 3rd November 2025

DOI: 10.1039/d5ra05096k

rsc.li/rsc-advances

In this study, a rapid and sensitive UHPLC-ESI-QTOF-MS/MS method was established to characterize and differentiate saponin profiles in the leaves of *Ilex cochinchinensis*, *Ilex annamensis*, and *Ilex rotunda* collected in Vietnam. This is the first report on the chemical composition of *I. cochinchinensis* and *I. annamensis* using this advanced analytical approach. A total of 63 saponins were tentatively identified across all samples, with *I. cochinchinensis*, *I. annamensis*, and *I. rotunda* containing 39, 30, and 34 compounds, respectively. Among these, seven saponins were newly reported from *I. cochinchinensis*, including two novel structures corresponding to compound 9 at a retention time (RT) of 11.83 minutes, one novel structure corresponding to compound 15 at RT 12.09 minutes, and four novel structures corresponding to compound 46 at RT 13.71 minutes. Notably, compound 46 was also detected in *I. annamensis*, whereas no new saponins were identified in *I. rotunda*. Saponin profiles allowed clear differentiation among the three species. Additionally, we evaluated the tyrosinase inhibitory activity of methanolic leaf extracts at 100 μg mL^{-1}. *I. annamensis* exhibited the highest inhibition (40.70% ± 1.84), followed by *I. cochinchinensis* (24.40% ± 1.27) and *I. rotunda* (14.43% ± 1.53). These findings not only expand the phytochemical database of Vietnamese *Ilex* species but also highlight the potential of *I. annamensis* as a promising source of natural tyrosinase inhibitors for cosmetic and dermatological applications.

Introduction

Ilex, also known as holly, is the only genus still existing in the monogenetic family Aquifoliaceae and estimated to be at least 669 known *Ilex* species.[1] According to Plants of the World Online (POWO), *Ilex* is the second-largest genus of dioecious plants in the world after *Diospyros* L. which has 730 recognized species.[2] Numerous species in this genus were reported for potential pharmacological uses such as antimicrobial, anti-inflammatory, antioxidant activity, which could be used as anti-obesity, anti-diabetic agents. Thus, these species could be applied to treat a wide range of medical conditions.[1–7] The chemical compounds performing these functions were mentioned as terpenoids, saponins, polyphenols, flavonoids and phenolic glycosides.[3,5]

Among them, *Ilex rotunda* has been officially listed in the Chinese Pharmacopoeia 2020 and traditionally used by the Yao ethnic group for treating cardiovascular conditions. Modern pharmacological studies have reported its potential to reduce coronary artery flow, regulate heart rate, enhance hypoxia tolerance, and exhibit antiarrhythmic properties. A recent study identified 105 chemical compounds from the bark of *I. rotunda* using UPLC-QTOF-MS/MS (Chen *et al.*, 2021).[8] However, the chemical profile of *I. rotunda* cultivated in Vietnam remains poorly documented. Additionally, including *I. rotunda* in a comparative study with the lesser-known *Ilex* species provides valuable insights into differences in phytochemical composition and associated bioactivities.

Recently, UHPLC coupled with quadrupole time-of-flight mass spectrometry (QTOF-MS/MS) has become a powerful tool for rapid screening and identification of complex phytochemicals in natural products. For example, LC-QTOF-MS/MS has been successfully used to characterize 80 compounds from *Acer* species,[9] 65 metabolites in various berries,[10] 171 constituents in lotus plants,[11] 74 secondary metabolites from fruits, leaves, and flowers of *Forsythia suspensa*,[12] *etc.* Our research team also applied this technique to study the chemical composition of *Hedera helix* and *Hedera nepalensis* in Vietnam.[13–15]

[a]*Graduate University of Science and Technology, Vietnam Academy of Science and Technology (VAST), Ho Chi Minh City, Vietnam*

[b]*Institute of Advanced Technology, Vietnam Academy of Science and Technology (VAST), Ho Chi Minh City, Vietnam. E-mail: pvtrung@iat.vast.vn; trung_cnhh@yahoo.com*

[c]*Department of Biology, University of Dalat, Dalat, Vietnam*

Melanin is primarily responsible for determining skin color and pigmentation. Approximately 10% of the skin cells in the deepest layer of the epidermis are involved in the production of melanin. When the skin is exposed to UV light, the process of melanogenesis is triggered by an enzyme called tyrosinase.[16–18] This inspired scientists and researchers to concentrate on the discovery, synthesis, isolation, and characterisation of novel, highly effective tyrosinase inhibitors for use in the food,[19] cosmetics,[20] and medicinal industries.[21] Tyrosinase inhibitors such as kojic acid and hydroquinone, although originally derived from natural sources such as fungi and plants, are commonly synthesized for commercial applications, and their use has been associated with skin irritation.[16] Therefore, researchers are actively searching for alternatives, such as naturally derived chemicals for use in safer skin whitening products.

Although numerous studies have investigated the phytochemical composition and bioactivities of various *Ilex* species,[22–27] research on *Ilex cochinchinensis* and *Ilex annamensis* remains limited. In this study, we developed a straightforward, rapid, and sensitive UHPLC-ESI-QTOF-MS/MS method to identify and differentiate saponins from the leaf extracts of *I. cochinchinensis*, *I. annamensis*, and *I. rotunda* collected in Vietnam. Furthermore, the tyrosinase inhibitory activity of the leaf extracts from all three species was evaluated for the first time. These findings not only expand the phytochemical and biological knowledge of *Ilex* species in Vietnam but also support their potential applications in the development of natural tyrosinase inhibitors.

Results and discussion

Structural characterization of saponins by UHPLC-ESI-QTOF-MS/MS

The crude methanol extracts from leaves of *Ilex cochinchinensis* and *Ilex annamensis* were analyzed by UHPLC-ESI-QTOF-MS/MS in positive and negative ionization modes to comprehensively characterize the saponins in each part of the two species. The identification information was summarized in Table 1. The appearance of the saponins in each sample was presented in Table 2. Deprotonated ions $[M - H]^-$ and solvent adduct ions $[M + HCOO]^-$ can be observed in the negative ESI mode, while protonated ions $[M + H]^+$ and ammoniated ions $[M + NH_4]^+$ can be obtained in the positive ESI mode. Additionally, fragments representing dehydration and HCOOH loss from these aglycones can be easily observed in positive ESI mode. To facilitate structural elucidation, UPLC-ESI-QTOF-MS/MS data were interpreted in combination with previously reported fragmentation patterns of structurally related saponins. Previous reports, such as the comprehensive MS analysis of matesaponins from *Ilex paraguariensis*,[28] the dereplication of triterpenoid saponins from *Pulsatilla chinensis*,[29] and the recent characterisation of *Hedera nepalensis* saponins[30] have demonstrated characteristic fragmentation pathways: (i) preferential cleavage of glycosides at C-28 due to the labile ester linkage, (ii) stepwise loss of C-3 linked monosaccharides, and (iii) complementary evidence from both positive and negative ion modes. By following these established MS-based strategies, we tentatively identified the saponins in our study and provided supporting references in the revised manuscript.

The composition of the sugar chain can be inferred from the loss of specific fragment ions as follows: arabinopyranosyl (Ara) or xylopyranosyl (Xyl) loss is 132 Da, rhamnopyranosyl (Rha) loss is 146 Da, glucopyranosyl (Glc) or galactopyranosyl (Gal) loss is 162 Da, and glucuronopyranosyl (Glu) loss is 176 Da. Moreover, some functional groups including methyl, acetyl, 4-hydroxy-*E*-cinnamoyl were observed when analyzing the fragments.

In the three *Ilex* species, the identified saponins were found to contain triterpenoid aglycones primarily belonging to the ursane, oleanane, and taraxastene skeleton types, including (**A1**) 2,3,19,23-tetrahydroxy-12-ursen-28-oic acid; (2α,3β,19α,20β)-form (23-hydroxytormentic acid), (**A2**) 20-taraxastene-3,28-diol; 3β-form, 28-carboxylic acid (heterobetulinic acid), (**A3**) 3,19,24-trihydroxy-12-oleanen-28-oic acid; (3β,19α)-form (spathodic acid), (**A4**) 3,19,23-trihydroxy-12-ursen-28-oic acid; (3β,19α)-form (rotundic acid), (**A5**) 2,3,19,24-tetrahydroxy-12-oleanen-28-oic acid; (2α,3β,19α)-form (sericic acid), (**A6**) 3,19-dihydroxy-12-ursen-28-oic acid; (3β,19α)-form (pomolic acid), (**A7**) 3,19-dihydroxy-12-ursene-24,28-dioic acid; (3β,19α)-form (Ilexgenin A), (**A8**) 3,19,23,30-tetrahydroxy-12-ursen-28-oic acid; (3β,19α)-form (30-hydroxyrotundic acid), (**A9**) 3,19-dihydroxy-12-ursen-28-oic acid; (3β,19α,20β)-form (Ilexgenin B), (**A10**) 3,19,23-trihydroxy-12,20(30)-ursadien-28-oic acid; (3β,19α)-form, (**A11**) 3,19,24-trihydroxy-12-ursen-28-oic acid; (3β,19α)-form (rotungenic acid), (**A12**) 3,11,19,20-tetrahydroxy-13(18)-ursen-28-oic acid; (3β,11β,19α,20β)-form, with a 28→20 lactone (γ-kudinlactone), (**A13**) 3,23-dihydroxy-12,18-ursadien-28-oic acid; (3β,20β)-form, (**A14**) hederagenin, (**A15**) 3-hydroxy-19-oxo-19,20-seco-13(18)-ursen-28,20-olide; (3β,20S)-form (kudinone G), (**A16**) 3,12,19,20-tetrahydroxy-13(18)-ursen-28-oic acid; (3β,12β,19α,20β)-form, with a 28→20 lactone (β-kudinlactone), (**A17**) 3,23-dihydroxy-12-ursen-28-oic acid; (3β,20α)-form, (**A18**) 3,19-dihydroxy-24-nor-4(23),12-ursadien-28-oic acid; (3β,19α)-form, (**A19**) 3-hydroxy-12,19-ursadien-28-oic acid; 3β-form (tomentosolic acid), (**A20**) 3,19,20-trihydroxy-12-ursen-28-oic acid; (3β,19α,20β)-form, with a 28→20 lactone, (**A21**) 3,19-dihydroxy-12-oleanen-28-oic acid; (3β,19α)-form (siaresinolic acid), (**A22**) 3-hydroxy-12,18-ursadien-28-oic acid; (3β,20β)-form, (**A23**) 3-hydroxy-12-ursen-28-oic acid; 3β-form (ursolic acid), (**A24**) 3-hydroxy-12,18-ursadien-28-oic acid; 3β-form (ilexolic acid), (**A25**) 3,24-dihydroxy-12-ursen-28-oic acid; 3β-form, (**A26**) 3,27-dihydroxy-12-ursen-28-oic acid; 3β-form (27-hydroxyursolic acid), (**A27**) 12-ursene-3,11,16,28-tetrol; (3β,11α,16α)-form, and (**A28**) 12-ursene-3,11,28-triol; (3β,11α)-form, with an 11-ketone.

All saponins aglycones in *Ilex cochinchinensis*, *Ilex annamensis*, and *Ilex rotunda* leaves were illustrated in Fig. 1. Their structural moieties (aglycones and sugar chains) were shown in Table 3.

Using UHPLC-ESI-QTOF-MS/MS analysis, a total of eleven saponins were identified across all three *Ilex* species, corresponding to compounds 10, 12, 19, 20, 22, 25, 29, 31, 51, 60, and 63. In addition, fourteen saponins were found exclusively in the

Table 1 Identification of the chemical constituents of *Ilex cochinchinensis*, *Ilex annamensis*, and *Ilex rotunda* leaves by UPLC-Q-TOF-MS/MS

No.	RT	Precursor Mass	*m/z* Calculated	Error	Ion	Chemical name	Putative structure	MS/MS	Formula
1	11.08	711.3985	711.3956	−4.12	$[M + HCOO]^-$	2,3,19,23-Tetrahydroxy-12-ursen-28-oic acid; (2α,3β,19α,20β)-form, 28-*O*-β-D-glucopyranosyl ester	**A1**–Glc	665.3876 $[M - H]^-$ 503.3356 $[M - H–Glc]^-$	$C_{36}H_{58}O_{11}$
2	11.12	751.4632	751.4633	0.07	$[M + H]^+$	20-Taraxastene-3,28-diol; 3β-form, 28-carboxylic acid, 3-*O*-[β-D-glucopyranosyl-(1→2)-β-D-xylopyranoside]	Glc–Xyl–**A2**	457.3684 $[M + H–Glc–Xyl]^+$	$C_{41}H_{66}O_{12}$
3	11.13	665.3909	665.3901	−1.22	$[M + H]^+$	3,19,24-Trihydroxy-12-oleanen-28-oic acid; (3β,19α)-form, 3-*O*-β-D-glucuronopyranoside	Glu–**A3**	489.3561 $[M + H–Glu]^+$	$C_{36}H_{56}O_{11}$
4	11.24	857.4574	857.4535	−4.57	$[M + HCOO]^-$	3,19,23-Trihydroxy-12-ursen-28-oic acid; (3β,19α)-form, 3-*O*-β-D-glucopyranoside, 28-*O*-β-D-glucopyranosyl ester	Glc–**A4**–Glc	811.4497 $[M - H]^-$ 649.3924 $[M - H–Glc]^-$ 487.3403 $[M - H–2Glc]^-$	$C_{42}H_{68}O_{15}$
5	11.41	825.4299	825.4273	−3.19	$[M - H]^-$	3,19,23-Trihydroxy-12-ursen-28-oic acid; (3β,19α)-form, 3-*O*-β-D-glucuronopyranoside, 28-*O*-β-D-glucopyranosyl ester	Glu–**A4**–Glc	663.3718 $[M - H–Glc]^-$ 487.3434 $[M - H–Glc–Glu]^-$	$C_{42}H_{66}O_{16}$
6	11.44	695.4039	695.4007	−4.67	$[M + HCOO]^-$	3,19,23-Trihydroxy-12-ursen-28-oic acid; (3β,19α)-form, 3-*O*-β-D-glucopyranoside	Glc–**A4**	649.3938 $[M - H]^-$ 487.3412 $[M - H–Glc]^-$	$C_{36}H_{58}O_{10}$
7	11.74	827.4447	827.4429	−2.16	$[M + HCOO]^-$	3,19,23-Trihydroxy-12-ursen-28-oic acid; (3β,19α)-form, 3-*O*-α-L-arabinopyranoside, 28-*O*-β-D-glucopyranosyl ester	Ara–**A4**–Glc	781.4348 $[M - H]^-$ 619.3820 $[M - H–Glc]^-$ 487.3438 $[M - H–Glc–Ara]^-$	$C_{41}H_{66}O_{14}$
8	11.82	667.4069	667.4057	−1.74	$[M + H]^+$	2,3,19,24-Tetrahydroxy-12-oleanen-28-oic acid; (2α,3β,19α)-form, 28-*O*-β-D-glucopyranosyl ester	**A5**–Glc	505.3551 $[M + H–Glc]^+$	$C_{36}H_{58}O_{11}$
9	11.83	959.5243	959.5216	−2.86	$[M + HCOO]^-$	12-ursene-3,11,16,28-tetrol; (3β,11α,16α)-form, 3-*O*-[β-D-glucopyranosyl-(1→3)-α-L-rhamnopyranosyl-(1→2)-α-L-arabinopyranoside] OR 12-ursene-3,11,16,28-tetrol; (3β,11α,16α)-form, 3-*O*-[β-D-glucopyranosyl-(1→3)-[α-L-rhamnopyranosyl-(1→2)]-α-L-arabinopyranoside]	Glc–Rha–Ara–**A27** Or Glc-Ara-**A27** | Rha	913.5132 $[M - H]^-$ 751.4598 $[M - H–Glc]^-$ 605.4026 $[M - H–Glc–Rha]^-$ 473.3607 $[M - H–Glc–Rha–Ara]^-$	$C_{47}H_{78}O_{17}$
10	11.93	809.4355	809.4324	−3.89	$[M - H]^-$	3,19-Dihydroxy-12-ursen-28-oic acid; (3β,19α)-form, 3-*O*-β-D-glucuronopyranoside, 28-*O*-β-D-glucopyranosyl ester	Glu–**A6**–Glc	647.3771 $[M - H–Glc]^-$ 471.3454 $[M - H–Glc–Glu]^-$	$C_{42}H_{66}O_{15}$

Table 1 (*Contd.*)

No.	RT	Precursor Mass	*m*/*z* Calculated	Error	Ion	Chemical name	Putative structure	MS/MS	Formula
11	11.94	709.3821	709.3799	−3.07	$[M + HCOO]^-$	3,19-Dihydroxy-12-ursene-24,28-dioic acid; (3β,19α)-form, 28-*O*-β-D-glucopyranosyl ester	**A7**–Glc	663.3744 $[M - H]^-$ 501.3195 $[M - H–Glc]^-$	$C_{36}H_{56}O_{11}$
12	12.01	668.4373	668.4374	0.11	$[M + NH_4]^+$	3,19,24-Trihydroxy-12-oleanen-28-oic acid; (3β,19α)-form, 28-*O*-β-D-glucopyranosyl ester	**A3**–Glc	489.3584 $[M + H–Glc]^+$	$C_{36}H_{58}O_{10}$
13	12.06	973.5047	973.5008	−3.98	$[M + HCOO]^-$	3,19-Dihydroxy-12-ursen-28-oic acid; (3β,19α)-form, 3-*O*-[β-D-glucopyranosyl-(1→2)-α-L-arabinopyranoside], 28-*O*-β-D-glucopyranosyl ester	Glc–Ara–**A6**–Glc	927.4918 $[M - H]^-$ 765.4394 $[M - H–Glc]^-$ 603.3873 $[M - H–2Glc]^-$ 471.3451 $[M - H–2Glc–Ara]^-$	$C_{47}H_{76}O_{18}$
14	12.07	711.3991	711.3956	−4.96	$[M + HCOO]^-$	3,19,23,30-Tetrahydroxy-12-ursen-28-oic acid; (3β,19α)-form, 28-*O*-β-D-glucopyranosyl ester	**A8**–Glc	665.3872 $[M - H]^-$ 503.3348 $[M - H–Glc]^-$	$C_{36}H_{58}O_{11}$
15	12.09	813.4647	813.4637	−1.29	$[M + HCOO]^-$	12-ursene-3,11,16,28-tetrol; (3β,11α,16α)-form, 3-*O*-[β-D-glucopyranosyl-(1→2)-α-L-arabinopyranoside]	Glc–Ara–**A27**	767.4548 $[M - H]^-$ 605.4023 $[M - H–Glc]^-$ 473.3617 $[M - H–Glc–Ara]^-$	$C_{41}H_{68}O_{13}$
16	12.17	784.4840	784.4847	0.92	$[M + NH_4]^+$	3,19-Dihydroxy-12-ursen-28-oic acid; (3β,19α,20β)-form, 3-*O*-[β-D-glucopyranosyl-(1→3)-α-L-arabinopyranoside]	Glc–Ara–**A9**	605.4081 $[M + H–Glc]^+$ 473.3653 $[M + H–Glc–Ara]^+$	$C_{41}H_{66}O_{13}$
17	12.28	693.3877	693.3850	−3.89	$[M + HCOO]^-$	3,19,23-Trihydroxy-12,20(30)-ursadien-28-oic acid; (3β,19α)-form, 28-*O*-β-D-glucopyranosyl ester	**A10**–Glc	647.3764 $[M - H]^-$ 485.3245 $[M - H–Glc]^-$	$C_{36}H_{56}O_{10}$
18	12.35	1265.6171	1265.6166	−0.36	$[M + HCOO]^-$	3,19-Dihydroxy-12-ursen-28-oic acid; (3β,19α,20β)-form, 3-*O*-[α-L-rhamnopyranosyl-(1→2)-[β-D-glucopyranosyl-(1→3)]-α-L-arabinopyranoside], 28-*O*-[α-L-rhamnopyranosyl-(1→2)-β-D-glucopyranosyl] ester	Rha-Ara-**A9**-Glc-Rha | Glc	1219.6023 $[M - H]^-$ 911.5003 $[M - H–Rha–Glc]^-$ 749.4495 $[M - H–Rha–2Glc]^-$ 603.3924 $[M - H–2Rha–2Glc]^-$ 471.3465 $[M - H–2Rha–2Glc–Ara]^-$	$C_{59}H_{96}O_{26}$
19	12.45	695.4008	695.4007	−0.21	$[M + HCOO]^-$	3,19,23-Trihydroxy-12-ursen-28-oic acid; (3β,19α)-form, 28-*O*-β-D-glucopyranosyl ester	**A4**–Glc	649.3926 $[M - H]^-$ 487.3403 $[M - H–Glc]^-$	$C_{36}H_{58}O_{10}$

Table 1 (*Contd.*)

No.	RT	Precursor Mass	*m*/*z* Calculated	Error	Ion	Chemical name	Putative structure	MS/MS	Formula
20	12.53	957.5087	957.5059	−2.91	$[M + HCOO]^-$	3,19-Dihydroxy-12-ursen-28-oic acid; (3β,19α,20β)-form, 3-*O*-[α-L-rhamnopyranosyl-(1→2)-α-L-arabinopyranoside], 28-*O*-β-D-glucopyranosyl ester	Rha–Ara–**A9**–Glc	911.4975 $[M - H]^-$ 749.4451 $[M - H–Glc]^-$ 603.3886 $[M - H–Glc–Rha]^-$ 471.3451 $[M - H–Glc–Rha–Ara]^-$	$C_{47}H_{76}O_{17}$
21	12.56	1103.5644	1103.5638	−0.53	$[M + HCOO]^-$	3,19-Dihydroxy-12-ursen-28-oic acid; (3β,19α)-form, 3-*O*-[α-L-rhamnopyranosyl-(1→2)-α-L-arabinopyranoside], 28-*O*-[α-L-rhamnopyranosyl-(1→2)-β-D-glucopyranosyl] ester	Rha–Ara–**A6**–Glc–Rha	1057.5583 $[M - H]^-$ 749.4476 $[M - H–Glc–Rha]^-$ 603.3897 $[M - H–Glc–2Rha]^-$ 471.3474 $[M - H–Glc–2Rha–Ara]^-$	$C_{53}H_{86}O_{21}$
22	12.58	841.4589	841.4586	−0.40	$[M + HCOO]^-$	3,19,24-Trihydroxy-12-ursen-28-oic acid; (3β,19α)-form, 28-*O*-[α-L-rhamnopyranosyl-(1→2)-β-D-glucopyranosyl] ester	**A11**–Glc–Rha	795.4497 $[M - H]^-$ 487.3412 $[M - H–Glc–Rha]^-$	$C_{42}H_{68}O_{14}$
23	12.67	1119.5582	1119.5587	0.48	$[M + HCOO]^-$	3,19-Dihydroxy-12-ursen-28-oic acid; (3β,19α)-form, 3-*O*-[β-D-glucopyranosyl-(1→2)-β-D-glucopyranosyl-(1→3)-[α-L-rhamnopyranosyl-(1→2)]-α-L-arabinopyranoside]	Glc-Glc-Ara-**A6** | Rha	1073.5495 $[M - H]^-$ 911.5000 $[M - H–Glc]^-$ 749.4452 $[M - H–2Glc]^-$ 603.3868 $[M - H–2Glc–Rha]^-$ 471.3451 $[M - H–2Glc–Rha–Ara]^-$	$C_{53}H_{86}O_{22}$
24	12.70	971.4869	971.4852	−1.78	$[M + HCOO]^-$	3,11,19,20-Tetrahydroxy-13(18)-ursen-28-oic acid; (3β,11β,19α,20β)-form, 28→20 lactone, 3-*O*-[α-L-rhamnopyranosyl-(1→2)-[β-D-glucopyranosyl-(1→3)]-α-L-arabinopyranoside]	Rha-Ara-**A12** | Glc	925.4784 $[M - H]^-$ 763.4247 $[M - H–Glc]^-$ 617.3700 $[M - H–Glc–Rha]^-$ 485.3243 $[M - H–Glc–Rha–Ara]^-$	$C_{47}H_{74}O_{18}$
25	12.74	955.4943	955.4903	−4.23	$[M - H]^-$	3,19-Dihydroxy-12-ursen-28-oic acid; (3β,19α)-form, 3-*O*-[α-L-arabinopyranosyl-(1→2)-6-*O*-methyl-β-D-glucuronopyranoside], 28-*O*-β-D-glucopyranosyl ester	Ara–methyl Glu–**A6**–Glc	793.4388 $[M - H–Glc]^-$ 661.3918 $[M - H–Glc–Ara]^-$ 471.3497 $[M - H–Glc–Ara–methyl Glu]^-$	$C_{48}H_{76}O_{19}$
26	12.77	713.3583	713.3571	−1.72	$[M - H]^-$	3,19-Dihydroxy-12-ursen-28-oic acid; (3β,19α)-form, 3-sulfate, 28-*O*-β-D-glucopyranosyl ester	sulfate–**A6**–Glc	551.3015 $[M - H–Glc]^-$ 471.3478 $[M - H–Glc–SO_3H]^-$	$C_{36}H_{58}O_{12}S$

Table 1 (*Contd.*)

No.	RT	Precursor Mass	*m*/*z* Calculated	Error	Ion	Chemical name	Putative structure	MS/MS	Formula
27	12.83	647.3805	647.3795	−1.51	$[M + H]^+$	3,23-Dihydroxy-12,18-ursadien-28-oic acid; (3β,20β)-form, 3-*O*-β-D-glucuronopyranoside	Glu–**A13**	471.3453 $[M + H–Glu]^+$	$C_{36}H_{54}O_{10}$
28	12.84	839.4426	839.4429	0.38	$[M + HCOO]^-$	3,11,19,20-Tetrahydroxy-13(18)-ursen-28-oic acid; (3β,11β,19α,20β)-form, 28→20 lactone, 3-*O*-[α-L-rhamnopyranosyl-(1→2)-β-D-glucopyranoside]	Rha–Glc–**A12**	793.4352 $[M - H]^-$ 485.3269 $[M - H–Glc–Rha]^-$	$C_{42}H_{66}O_{14}$
29	12.89	809.4360	809.4324	−4.51	$[M - H]^-$	Hederagenin bisdesmosides; diglycosides, 3-*O*-β-D-glucuronopyranoside, 28-*O*-β-D-glucopyranosyl ester	Glu–**A14**–Glc	647.3787 $[M - H–Glc]^-$ 471.3458 $[M - H–Glc–Glu]^-$	$C_{42}H_{66}O_{15}$
30	13.01	665.3929	665.3901	−4.22	$[M + HCOO]^-$	3,19,23-Trihydroxy-12-ursen-28-oic acid; (3β,19α)-form, 3-*O*-α-L-arabinopyranoside	Ara–**A4**	619.3844 $[M - H]^-$ 487.3445 $[M - H–Ara]^-$ 909.4812 $[M - H]^-$	$C_{35}H_{56}O_9$
31	13.03	955.4909	955.4903	−0.67	$[M + HCOO]^-$	3-Hydroxy-19-oxo-19,20-seco-13(18)-ursen-28,20-olide; (3β,20*S*)-form, 3-*O*-[α-L-rhamnopyranosyl-(1→2)-[β-D-glucopyranosyl-(1→3)]-α-L-arabinopyranoside]	Rha-Ara-**A15** | Glc	747.4304 $[M - H–Glc]^-$ 601.3720 $[M - H–Glc–Rha]^-$ 469.3346 $[M - H–Glc–Rha–Ara]^-$	$C_{47}H_{74}O_{17}$
32	13.06	695.4017	695.4007	−1.50	$[M + HCOO]^-$	3,19,24-Trihydroxy-12-ursen-28-oic acid; (3β,19α)-form, 28-*O*-β-D-glucopyranosyl ester	**A11**–Glc	649.3926 $[M - H]^-$ 487.3412 $[M - H–Glc]^-$	$C_{36}H_{58}O_{10}$
33	13.09	649.3969	649.3952	−2.66	$[M + HCOO]^-$	3,19-Dihydroxy-12-ursen-28-oic acid; (3β,19α)-form, 3-*O*-α-L-arabinoside	Ara–**A6**	603.3872 $[M - H]^-$ 471.3456 $[M - H–Ara]^-$	$C_{35}H_{56}O_8$
34	13.17	784.4838	784.4847	1.17	$[M + NH_4]^+$	3,19-Dihydroxy-12-ursen-28-oic acid; (3β,19α,20β)-form, 3-*O*-α-L-arabinopyranoside, 28-*O*-β-D-glucopyranosyl ester	Ara–**A9**–Glc	635.4134 $[M + H–Ara]^+$ 473.3646 $[M + H–Ara–Glc]^+$	$C_{41}H_{66}O_{13}$
35	13.23	763.4288	763.4269	−2.53	$[M - H]^-$	3,12,19,20-Tetrahydroxy-13(18)-ursen-28-oic acid; (3β,12β,19α,20β)-form, (28→20)-lactone, 3-*O*-[α-L-rhamnopyranosyl-(1→2)-α-L-arabinopyranoside]	Rha–Ara–**A16**	617.3636 $[M - H–Rha]^-$ 485.3184 $[M - H–Rha–Ara]^-$	$C_{41}H_{64}O_{13}$
36	13.26	663.3767	663.3744	−3.41	$[M - H]^-$	3,19,23-Trihydroxy-12-ursen-28-oic acid; (3β,19α)-form, 3-*O*-β-D-glucuronopyranoside	Glu–**A4**	487.3419 $[M - H–Glu]^-$	$C_{36}H_{56}O_{11}$

Table 1 (*Contd.*)

No.	RT	Precursor Mass	*m*/*z* Calculated	Error	Ion	Chemical name	Putative structure	MS/MS	Formula
37	13.27	911.5036	911.5004	−3.48	$[M - H]^-$	3-Hydroxy-12-ursen-28-oic acid; 3β-form, 3-*O*-[β-D-glucopyranosyl-(1→3)-α-L-arabinopyranoside], 28-*O*-β-D-glucopyranosyl ester	Glc–Ara–**A23**–Glc	749.4453 [M − H–Glc]$^-$ 587.3956 [M − H-2Glc]$^-$ 455.3503 [M − H-2Glc–Ara]$^-$	$C_{47}H_{76}O_{17}$
38	13.29	987.4827	987.4801	−2.64	$[M + HCOO]^-$	3,19-Dihydroxy-12-ursen-28-oic acid; (3β,19α)-form, 3-*O*-[α-L-arabinopyranosyl-(1→2)-β-D-glucuronopyranoside], 28-*O*-β-D-glucopyranosyl ester	Ara–Glu–**A6**–Glc	941.4704 [M − H]$^-$ 779.4177 [M − H–Glc]$^-$ 647.3763 [M − H–Glc–Ara]$^-$ 471.3472 [M − H–Glc–Ara–Glu]$^-$	$C_{47}H_{74}O_{19}$
39	13.38	957.5077	957.5059	−1.87	$[M + HCOO]^-$	3,19-Dihydroxy-12-ursen-28-oic acid; (3β,19α)-form, 3-*O*-[α-L-rhamnopyranosyl-(1→2)-α-L-arabinopyranoside], 28-*O*-β-D-glucopyranosyl ester	Rha–Ara–**A6**–Glc	911.4966 [M − H]$^-$ 749.4442 [M − H–Glc]$^-$ 603.3867 [M − H–Glc–Rha]$^-$ 471.3485 [M − H–Glc–Rha–Ara]$^-$	$C_{47}H_{76}O_{17}$
40	13.43	665.3916	665.3901	−2.27	$[M + H]^+$	3,19,24-Trihydroxy-12-ursen-28-oic acid; (3β,19α)-form, 3-*O*-β-D-glucuronopyranoside	Glu–**A11**	489.3596 [M + H–Glu]$^+$	$C_{36}H_{56}O_{11}$
41	13.43	693.3861	693.3850	−1.58	$[M + HCOO]^-$	3,12,19,20-Tetrahydroxy-13(18)-ursen-28-oic acid; (3β,12β,19α,20β)-form, (28→20)-lactone, 3-*O*-β-D-glucopyranoside	Glc–**A16**	647.3795 [M − H]$^-$ 485.3267 [M − H–Glc]$^-$	$C_{36}H_{56}O_{10}$
42	13.43	839.4448	839.4429	−2.25	$[M + HCOO]^-$	3,12,19,20-Tetrahydroxy-13(18)-ursen-28-oic acid; (3β,12β,19α,20β)-form, (28→20)-lactone, 3-*O*-[α-L-rhamnopyranosyl-(1→2)-β-D-glucopyranoside]	Rha–Glc–**A16**	793.4345 [M − H]$^-$ 485.3241 [M − H–Glc–Rha]$^-$	$C_{42}H_{66}O_{14}$
43	13.48	971.4856	971.4852	−0.44	$[M + HCOO]^-$	3,12,19,20-Tetrahydroxy-13(18)-ursen-28-oic acid; (3β,12β,19α,20β)-form, (28→20)-lactone, 3-*O*-[β-D-glucopyranosyl-(1→3)-[α-L-rhamnopyranosyl-(1→2)]-α-L-arabinopyranoside]	Glc-Ara-**A16** | Rha	925.4753 [M − H]$^-$ 763.4231 [M − H–Glc]$^-$ 617.3689 [M − H–Glc–Rha]$^-$ 485.3249 [M − H–Glc–Rha–Ara]$^-$	$C_{47}H_{74}O_{18}$

Table 1 (*Contd.*)

No.	RT	Precursor Mass	*m*/*z* Calculated	Error	Ion	Chemical name	Putative structure	MS/MS	Formula
44	13.54	784.4851	784.4847	−0.49	$[M + NH_4]^+$	3,23-Dihydroxy-12-ursen-28-oic acid; (3β,20α)-form, 3-*O*-α-L-arabinopyranoside, 28-*O*-β-D-glucopyranosyl ester	Ara–**A17**–Glc	635.4134 [M + H–Ara]$^+$ 473.3608 [M + H–Ara–Glc]$^+$	
45	13.54	1133.5387	1133.5380	−0.62	$[M + HCOO]^-$	3,12,19,20-Tetrahydroxy-13(18)-ursen-28-oic acid; (3β,12β,19α,20β)-form, (28→20)-lactone, 3-*O*-[β-D-glucopyranosyl-(1→2)-β-D-glucopyranosyl-(1→3)-[α-L-rhamnopyranosyl-(1→2)]-α-L-arabinopyranoside]	Glc-Glc-Ara-**A16** | Rha	1087.5378 [M − H]$^-$ 925.4779 [M − H–Glc]$^-$ 763.4226 [M − H–2Glc]$^-$ 485.3238 [M − H–2Glc–Rha–Ara]$^-$	$C_{41}H_{66}O_{13}$ $C_{53}H_{84}O_{23}$
46	13.71	941.5124	941.5110	−1.49	$[M + HCOO]^-$	12-ursene-3,11,28-triol; (3β,11α)-form, 11-ketone, 3-*O*-[β-D-glucopyranosyl-(1→2)-α-L-arabinopyranosyl-(1→2)-α-L-rhamnopyranoside OR 12-ursene-3,11,28-triol; (3β,11α)-form, 11-ketone, 3-*O*-[β-D-glucopyranosyl-(1→3)-[α-L-arabinopyranosyl-(1→2)]-α-L-rhamnopyranoside OR ursolic acid, 3-*O*-[β-D-glucopyranosyl-(1→2)-α-L-arabinopyranosyl-(1→2)-α-L-rhamnopyranoside] OR ursolic acid, 3-*O*-[β-D-glucopyranosyl-(1→3)-[α-L-arabinopyranosyl-(1→2)]-α-L-rhamnopyranoside]	Glc–Ara–Rha–**A28** Or Glc-Rha-**A28** | Ara Or Glc–Ara–Rha–**A23** Or Glc-Rha-**A23** | Ara	895.5014 [M − H]$^-$ 733.4492 [M − H–Glc]$^-$ 601.4092 [M − H–Glc–Ara]$^-$ 455.3528 [M − H–Glc–Ara–Rha]$^-$	$C_{47}H_{76}O_{16}$
47	13.77	663.3772	663.3744	−4.16	$[M + HCOO]^-$	3,19-Dihydroxy-24-nor-4(23),12-ursadien-28-oic acid; (3β,19α)-form, 28-*O*-β-D-glucopyranosyl ester	**A18**–Glc	617.3666 [M − H]$^-$ 455.3157 [M − H–Glc]$^-$	$C_{35}H_{54}O_9$
48	13.84	955.4925	955.4903	−2.34	$[M + HCOO]^-$	3-Hydroxy-12,19-ursadien-28-oic acid; 3β-form, 3-*O*-[β-D-glucopyranosyl-(1→2)-β-D-xylopyranoside], 28-*O*-β-D-glucopyranosyl ester	Glc–Xyl–**A19**–Glc	909.4803 [M − H]$^-$ 747.4293 [M − H–Glc]$^-$ 585.3762 [M − H–2Glc]$^-$ 453.3341 [M − H–2Glc–Xyl]$^-$	$C_{47}H_{74}O_{17}$
49	13.86	811.4514	811.4480	−4.19	$[M + HCOO]^-$	3,19-Dihydroxy-12-ursen-28-oic acid; (3β,19α)-form, 3-*O*-[β-D-glucopyranosyl-(1→2)-α-L-arabinopyranoside]	Glc–Ara–**A6**	765.4393 [M − H]$^-$ 603.3877 [M − H–Glc]$^-$ 471.3456 [M − H–Glc–Ara]$^-$	$C_{41}H_{66}O_{13}$

Table 1 (*Contd.*)

No.	RT	Precursor Mass	*m*/*z* Calculated	Error	Ion	Chemical name	Putative structure	MS/MS	Formula
50	13.90	957.5077	957.5059	−1.87	$[M + HCOO]^-$	3,19-Dihydroxy-12-ursen-28-oic acid; (3β,19α)-form, 3-*O*-[α-L-rhamnopyranosyl-(1→2)-β-D-glucopyranosyl-(1→2)-α-L-arabinopyranoside]	Rha–Glc–Ara–**A6**	911.4965 $[M - H]^-$ 765.4397 $[M - H$–Rha$]^-$ 603.3878 $[M - H$–Rha–Glc$]^-$ 471.3451 $[M - H$–Rha–Glc–Ara$]^-$	$C_{47}H_{76}O_{17}$
51	14.19	647.3800	647.3795	−0.73	$[M - H]^-$	3,19-Dihydroxy-12-ursen-28-oic acid; (3β,19α)-form, 3-*O*-β-D-glucuronopyranoside	Glu–**A6**	471.3453 $[M - H$–Glu$]^-$	$C_{36}H_{56}O_{10}$
52	14.32	825.4296	825.4273	−2.83	$[M + HCOO]^-$	3,19-Dihydroxy-12-ursen-28-oic acid; (3β,19α)-form, 3-*O*-[α-L-arabinopyranosyl-(1→2)-β-D-glucuronopyranoside]	Ara–Glu–**A6**	779.4193 $[M - H]^-$ 471.3450 $[M - H$–Ara–Glu$]^-$	$C_{41}H_{64}O_{14}$
53	14.57	647.3790	647.3795	0.81	$[M + HCOO]^-$	3,23-Dihydroxy-12,18-ursadien-28-oic acid; (3β,20β)-form, 3-*O*-α-L-arabinopyranoside	Ara–**A13**	601.3740 $[M - H]^-$ 469.3295 $[M - H$–Ara$]^-$ 1071.5322 $[M - H]^-$	$C_{35}H_{54}O_8$
54	14.61	1117.5431	1117.5431	−0.01	$[M + HCOO]^-$	3,19,20-Trihydroxy-12-ursen-28-oic acid; (3β,19α,20β)-form, (28→20)-lactone, 3-*O*-[β-D-glucopyranosyl-(1→2)-β-D-glucopyranosyl-(1→3)-[α-L-rhamnopyranosyl-(1→2)]-α-L-arabinopyranoside]	Glc-Glc-Ara-**A20** | Rha	909.4851 $[M - H$–Glc$]^-$ 747.4310 $[M - H$–2Glc$]^-$ 601.3776 $[M - H$–2Glc–Rha$]^-$ 469.3345 $[M - H$–2Glc–Rha–Ara$]^-$	$C_{53}H_{84}O_{22}$
55	14.82	955.4900	955.4903	0.27	$[M + HCOO]^-$	3,19,20-Trihydroxy-12-ursen-28-oic acid; (3β,19α,20β)-form, (28→20)-lactone, 3-*O*-[β-D-glucopyranosyl-(1→3)-[α-L-rhamnopyranosyl-(1→2)]-α-L-arabinopyranoside]	Glc-Ara-**A20** | Rha	909.4796 $[M - H]^-$ 747.4296 $[M - H$–Glc$]^-$ 601.3745 $[M - H$–Glc–Rha$]^-$ 469.3346 $[M - H$–Glc–Rha–Ara$]^-$	$C_{47}H_{74}O_{17}$
56	15.12	647.3819	647.3795	−3.67	$[M - H]^-$	3,19-Dihydroxy-12-oleanen-28-oic acid; (3β,19α)-form, 3-*O*-β-D-glucuronopyranoside	Glu–**A21**	471.3473 $[M - H$-Glu$]^-$	$C_{36}H_{56}O_{10}$
57	15.21	645.4013	645.4003	−1.61	$[M - H]^-$	3,19-Dihydroxy-12-ursen-28-oic acid; (3β,19α)-form, 3-*O*-(2-*O*-Acetyl-β-D-xylopyranoside)	Acetyl Xyl–**A6**	471.3465 $[M - H$-acetyl Xyl$]^-$	$C_{37}H_{58}O_9$
58	15.32	585.3805	585.3791	−2.34	$[M - H]^-$	3-Hydroxy-12,18-ursadien-28-oic acid; (3β,20β)-form, 3-*O*-α-L-arabinopyranoside	Ara–**A22**	453.3367 $[M - H$–Ara$]^-$	$C_{35}H_{54}O_7$

Table 1 (*Contd.*)

No.	RT	Precursor Mass	*m/z* Calculated	Error	Ion	Chemical name	Putative structure	MS/MS	Formula
59	15.47	795.4548	795.4531	−2.16	$[M + HCOO]^-$	3-Hydroxy-12-ursen-28-oic acid; 3β-form, 3-*O*-[β-D-glucopyranosyl-(1→2)-α-L-arabinopyranoside]	Glc–Ara–**A23**	749.4451 $[M - H]^-$ 587.3922 $[M - H\text{-}Glc]^-$ 455.3508 $[M - H\text{-}Glc\text{–}Ara]^-$	$C_{41}H_{66}O_{12}$
60	15.77	631.3860	631.3846	−2.20	$[M + HCOO]^-$	3-Hydroxy-12,18-ursadien-28-oic acid; 3β-form, 3-*O*-β-D-xylopyranoside	Xyl-**A24**	453.3357 $[M - H\text{-}Xyl]^-$	$C_{35}H_{54}O_7$
61	16.08	779.4591	779.4582	−1.19	$[M - H]^-$	3-Hydroxy-12-ursen-28-oic acid; 3β-form, 3-*O*-[β-D-glucopyranosyl-(1→2)-β-D-galactopyranoside]	Glc–Gal–**A23**	455.3503 $[M - H\text{-}2Glc]^-$	$C_{42}H_{68}O_{13}$
62	17.31	617.3840	617.3842	0.35	$[M - H]^-$	3,24-Dihydroxy-12-ursen-28-oic acid; 3β-form, 24-*O*-(4-hydroxy-*E*-cinnamoyl)	**A25**-[24-*O*-(4-Hydroxy-*E*-cinnamoyl)]	471.3474 $[M - H\text{-}hydroxy\text{-}cinnamoyl]^-$	$C_{39}H_{54}O_6$
63	18.29	617.3852	617.3842	−1.60	$[M - H]^-$	3,27-Dihydroxy-12-ursen-28-oic acid; 3β-form, 27-*O*-(4-hydroxy-*E*-cinnamoyl)	**A26**-[27-*O*-(4-Hydroxy-*E*-cinnamoyl)]	471.3491 $[M - H\text{-}hydroxy\text{-}cinnamoyl]^-$	$C_{39}H_{54}O_6$

leaf extract of *Ilex cochinchinensis*, including compounds 2, 7, 9, 13, 15–17, 27, 34, 37, 39, 57, 59, and 61. Notably, the chemical structures of compounds 9 and 15 are reported here for the first time. In the methanolic leaf extract of *Ilex annamensis*, five saponins – compounds 3, 8, 26, 40, and 56 – were tentatively characterized. Furthermore, eighteen additional saponins were detected in two of the three *Ilex* species examined. Among these, compound 46, found in both *I. cochinchinensis* and *I. annamensis*, is newly reported in terms of its chemical structure. These findings significantly expand the current knowledge of saponin diversity and distribution within the *Ilex* genus and provide a valuable foundation for future pharmacological and phytochemical investigations. Fragmentation pathways of compounds 9, 15, and 46 were shown in Fig. 2–4.

Compound **9** yielded $[M + HCOO]^-$ ion at *m/z* 959.5243 and $[M + NH_4]^+$ ion at 932.5582, corresponding to molecular formula $C_{47}H_{78}O_{17}$. In the negative mode, compound **9** provided fragments at *m/z* 751, 605, and 473, indicated the consecutive loss of Glc, Rha, and Ara. Additionally, in the positive mode, fragment ions at *m/z* 753, 607, and 475 demonstrated that the sugar chain Glc–Rha–Ara was connected to the C-3 position of the aglycone. Moreover, the aglycone ion at *m/z* 475 suggested an additional 18 Da compared to a reported aglycone of other *Ilex* species, of which name was 12-ursene-3,21,28-triol; (3β,21α)-form (this aglycone had *m/z* at 457 in the positive mode). The 18 Da difference was consistent with the presence of a hydroxyl group (–OH), indicating that the aglycone of compound **9** may be a tetrol, supporting the possibility of the aglycone being named 12-ursene-3,11,16,28-tetrol; (3β,11α,16α)-form. As a result, compound 9 was tentatively identified as 12-ursene-3,11,16,28-tetrol; (3β,11α,16α)-form, 3-*O*-[β-D-glucopyranosyl-(1→3)-α-L-rhamnopyranosyl-(1→2)-α-L-arabinopyranoside] (**9A**) or 12-ursene-3,11,16,28-tetrol; (3β,11α,16α)-form, 3-*O*-[β-D-glucopyranosyl-(1→3)-[α-L-rhamnopyranosyl-(1→2)]-α-L-arabinopyranoside] (**9B**), of which structures have been published for the first time.

Compound **15** yielded a solvent adduct ion $[M + HCOO]^-$ at *m/z* 813.4647 and an ammoniated ion $[M + NH_4]^+$ at *m/z* 786.4983, corresponding to molecular formula $C_{41}H_{68}O_{13}$. In the negative mode, compound **15** showed fragments at *m/z* 605 and 473. In the positive mode, the fragment ions were at *m/z* 607 and 475. These data indicated the consecutive loss of a Glc and an Ara at C-3 position of the aglycone. Furthermore, this aglycone was similar with compound **9**, which was possibly named as 12-ursene-3,11,16,28-tetrol; (3β,11α,16α)-form. Hence, compound **15** was tentatively determined as 12-ursene-3,11,16,28-tetrol; (3β,11α,16α)-form, 3-*O*-[β-D-glucopyranosyl-(1→2)-α-L-arabinopyranoside], of which structure was firstly reported.

Compound **46** yielded a solvent adduct ion $[M + HCOO]^-$ at *m/z* 941.5124 and an ammoniated ion $[M + NH_4]^+$ at *m/z* 914.5482, corresponding to molecular formula $C_{47}H_{76}O_{16}$. In the negative mode, compound **46** showed fragments at *m/z* 733, 601, and 455. In the positive mode, the fragment ions were at *m/z* 735, 603, and 457. These fragmentation patterns indicated the sequential loss of glucose (Glc), arabinose (Ara), and rhamnose (Rha) units from the C-3 position of the triterpenoid aglycone.

Table 2 Chemicals constituent differentiation of *Ilex cochinchinensis*, *Ilex annamensis*, and *Ilex rotunda* leaves[a]

No.	Chemical name	Synonym	ICL	IAL	IRL
1	2,3,19,23-Tetrahydroxy-12-ursen-28-oic acid; (2α,3β,19α,20β)-form, 28-*O*-β-D-glucopyranosyl ester	20*S*-Nigaichigoside F1	+	+	–
2	20-Taraxastene-3,28-diol; 3β-form, 28-carboxylic acid, 3-*O*-[β-D-glucopyranosyl-(1→2)-β-D-xylopyranoside]	x	+	–	–
3	3,19,24-Trihydroxy-12-oleanen-28-oic acid; (3β,19α)-form, 3-*O*-β-D-glucuronopyranoside	Ilexpuson G	–	+	–
4	3,19,23-Trihydroxy-12-ursen-28-oic acid; (3β,19α)-form, 3-*O*-β-D-glucopyranoside, 28-*O*-β-D-glucopyranosyl ester	Ilexoside XXXVII	+	+	–
5	3,19,23-Trihydroxy-12-ursen-28-oic acid; (3β,19α)-form, 3-*O*-β-D-glucuronopyranoside, 28-*O*-β-D-glucopyranosyl ester	Ilexoside XXXIX	+	+	–
6	3,19,23-Trihydroxy-12-ursen-28-oic acid; (3β,19α)-form, 3-*O*-β-D-glucopyranoside	Ilexpernoside C	+	+	–
7	3,19,23-Trihydroxy-12-ursen-28-oic acid; (3β,19α)-form, 3-*O*-α-L-arabinopyranoside, 28-*O*-β-D-glucopyranosyl ester	Ilekudinoside D	+	–	–
8	2,3,19,24-Tetrahydroxy-12-oleanen-28-oic acid; (2α,3β,19α)-form, 28-*O*-β-D-glucopyranosyl ester	Sericoside	–	+	–
9	12-ursene-3,11,16,28-tetrol; (3β,11α,16α)-form, 3-*O*-[β-D-glucopyranosyl-(1→3)-α-L-rhamnopyranosyl-(1→2)-α-L-arabinopyranoside] OR 12-ursene-3,11,16,28-tetrol; (3β,11α,16α)-form, 3-*O*-[β-D-glucopyranosyl-(1→3)-[α-L-rhamnopyranosyl-(1→2)]-α-L-arabinopyranoside]	x	+	–	–
10	3,19-Dihydroxy-12-ursen-28-oic acid; (3β,19α)-form, 3-*O*-β-D-glucuronopyranoside, 28-*O*-β-D-glucopyranosyl ester	Ilekudinoside B	+	+	+
11	3,19-Dihydroxy-12-ursene-24,28-dioic acid; (3β,19α)-form, 28-*O*-β-D-glucopyranosyl ester	x	–	–	+
12	3,19,24-Trihydroxy-12-oleanen-28-oic acid; (3β,19α)-form, 28-*O*-β-D-glucopyranosyl ester	x	+	+	+
13	3,19-Dihydroxy-12-ursen-28-oic acid; (3β,19α)-form, 3-*O*-[β-D-glucopyranosyl-(1→2)-α-L-arabinopyranoside], 28-*O*-β-D-glucopyranosyl ester	Ilexoside II	+	–	–
14	3,19,23,30-Tetrahydroxy-12-ursen-28-oic acid; (3β,19α)-form, 28-*O*-β-D-glucopyranosyl ester	Ilexoside XLIII	+	+	–
15	12-ursene-3,11,16,28-tetrol; (3β,11α,16α)-form, 3-*O*-[β-D-glucopyranosyl-(1→2)-α-L-arabinopyranoside]	x	+	–	–
16	3,19-Dihydroxy-12-ursen-28-oic acid; (3β,19α,20β)-form, 3-*O*-[β-D-glucopyranosyl-(1→3)-α-L-arabinopyranoside]	Ilemaminoside B	+	–	–
17	3,19,23-Trihydroxy-12,20(30)-ursadien-28-oic acid; (3β,19α)-form, 28-*O*-β-D-glucopyranosyl ester	Oblonganoside E	+	–	–
18	3,19-Dihydroxy-12-ursen-28-oic acid; (3β,19α,20β)-form, 3-*O*-[α-L-rhamnopyranosyl-(1→2)-[β-D-glucopyranosyl-(1→3)]-α-L-arabinopyranoside], 28-*O*-[α-L-rhamnopyranosyl-(1→2)-β-D-glucopyranosyl] ester	Latifoloside F	–	–	+
19	3,19,23-Trihydroxy-12-ursen-28-oic acid; (3β,19α)-form, 28-*O*-β-D-glucopyranosyl ester	Pedunculoside	+	+	+
20	3,19-Dihydroxy-12-ursen-28-oic acid; (3β,19α,20β)-form, 3-*O*-[α-L-rhamnopyranosyl-(1→2)-α-L-arabinopyranoside], 28-*O*-β-D-glucopyranosyl ester	Latifoloside D	+	+	+
21	3,19-Dihydroxy-12-ursen-28-oic acid; (3β,19α)-form, 3-*O*-[α-L-rhamnopyranosyl-(1→2)-α-L-arabinopyranoside], 28-*O*-[α-L-rhamnopyranosyl-(1→2)-β-D-glucopyranosyl] ester	Ilekudinoside W	–	–	+
22	3,19,24-Trihydroxy-12-ursen-28-oic acid; (3β,19α)-form, 28-*O*-[α-L-rhamnopyranosyl-(1→2)-β-D-glucopyranosyl] ester	x	+	+	+
23	3,19-Dihydroxy-12-ursen-28-oic acid; (3β,19α)-form, 3-*O*-[β-D-glucopyranosyl-(1→2)-β-D-glucopyranosyl-(1→3)-[α-L-rhamnopyranosyl-(1→2)]-α-L-arabinopyranoside]	Latifoloside L	–	–	+
24	3,11,19,20-Tetrahydroxy-13(18)-ursen-28-oic acid; (3β,11β,19α,20β)-form, 28→20 lactone, 3-*O*-[α-L-rhamnopyranosyl-(1→2)-[β-D-glucopyranosyl-(1→3)]-α-L-arabinopyranoside]	Kudinoside F	–	–	+
25	3,19-Dihydroxy-12-ursen-28-oic acid; (3β,19α)-form, 3-*O*-[α-L-arabinopyranosyl-(1→2)-6-*O*-methyl-β-D-glucuronopyranoside], 28-*O*-β-D-glucopyranosyl ester	x	+	+	+

Table 2 (*Contd.*)

No.	Chemical name	Synonym	ICL	IAL	IRL
26	3,19-Dihydroxy-12-ursen-28-oic acid; (3β,19α)-form, 3-sulfate, 28-*O*-β-D-glucopyranosyl ester	Ilexoside XXIX	–	+	–
27	3,23-Dihydroxy-12,18-ursadien-28-oic acid; (3β,20β)-form, 3-*O*-β-D-glucuronopyranoside	x	+	–	–
28	3,11,19,20-Tetrahydroxy-13(18)-ursen-28-oic acid; (3β,11β,19α,20β)-form, 28→20 lactone, 3-*O*-[α-L-rhamnopyranosyl-(1→2)-β-D-glucopyranoside]	Ilekudinoside S	–	–	+
29	Hederagenin bisdesmosides; Diglycosides, 3-*O*-β-D-glucuronopyranoside, 28-*O*-β-D-glucopyranosyl ester	Ilexoside XLVIII	+	+	+
30	3,19,23-Trihydroxy-12-ursen-28-oic acid; (3β,19α)-form, 3-*O*-α-L-arabinopyranoside	Mateside	+	+	–
31	3-Hydroxy-19-oxo-19,20-seco-13(18)-ursen-28,20-olide; (3β,20*S*)-form, 3-*O*-[α-L-rhamnopyranosyl-(1→2)-[β-D-glucopyranosyl-(1→3)]-α-L-arabinopyranoside]	Kudinoside LZ_{20}	+	+	+
32	3,19,24-Trihydroxy-12-ursen-28-oic acid; (3β,19α)-form, 28-*O*-β-D-glucopyranosyl ester	Rotungenoside	+	+	–
33	3,19-Dihydroxy-12-ursen-28-oic acid; (3β,19α)-form, 3-*O*-α-L-arabinoside	Ziyuglycoside II	–	+	+
34	3,19-Dihydroxy-12-ursen-28-oic acid; (3β,19α,20β)-form, 3-*O*-α-L-arabinopyranoside, 28-*O*-β-D-glucopyranosyl ester	Brevicuspisaponin 3	+	–	–
35	3,12,19,20-Tetrahydroxy-13(18)-ursen-28-oic acid; (3β,12β,19α,20β)-form, (28→20)-lactone, 3-*O*-[α-L-rhamnopyranosyl-(1→2)-α-L-arabinopyranoside]	Ilekudinoside R	–	–	+
36	3,19,23-Trihydroxy-12-ursen-28-oic acid; (3β,19α)-form, 3-*O*-β-D-glucuronopyranoside	Ilexpernoside D	+	+	–
37	3-Hydroxy-12-ursen-28-oic acid; 3β-form, 3-*O*-[β-D-glucopyranosyl-(1→3)-α-L-arabinopyranoside], 28-*O*-β-D-glucopyranosyl ester	Matesaponin 1	+	–	–
38	3,19-Dihydroxy-12-ursen-28-oic acid; (3β,19α)-form, 3-*O*-[α-L-arabinopyranosyl-(1→2)-β-D-glucuronopyranoside], 28-*O*-β-D-glucopyranosyl ester	x	–	–	+
39	3,19-Dihydroxy-12-ursen-28-oic acid; (3β,19α)-form, 3-*O*-[α-L-rhamnopyranosyl-(1→2)-α-L-arabinopyranoside], 28-*O*-β-D-glucopyranosyl ester	Latifoloside A	+	–	–
40	3,19,24-Trihydroxy-12-ursen-28-oic acid; (3β,19α)-form, 3-*O*-β-D-glucuronopyranoside	Ilexpuson F	–	+	–
41	3,12,19,20-Tetrahydroxy-13(18)-ursen-28-oic acid; (3β,12β,19α,20β)-form, (28→20)-lactone, 3-*O*-β-D-glucopyranoside	x	–	–	+
42	3,12,19,20-Tetrahydroxy-13(18)-ursen-28-oic acid; (3β,12β,19α,20β)-form, (28→20)-lactone, 3-*O*-[α-L-rhamnopyranosyl-(1→2)-β-D-glucopyranoside]	Ilekudinoside Q	–	–	+
43	3,12,19,20-Tetrahydroxy-13(18)-ursen-28-oic acid; (3β,12β,19α,20β)-form, (28→20)-lactone, 3-*O*-[β-D-glucopyranosyl-(1→3)-[α-L-rhamnopyranosyl-(1→2)]-α-L-arabinopyranoside]	Kudinoside A	–	+	+
44	3,23-Dihydroxy-12-ursen-28-oic acid; (3β,20α)-form, 3-*O*-α-L-arabinopyranoside, 28-*O*-β-D-glucopyranosyl ester	Mateglycoside C	+	–	+
45	3,12,19,20-Tetrahydroxy-13(18)-ursen-28-oic acid; (3β,12β,19α,20β)-form, (28→20)-lactone, 3-*O*-[β-D-glucopyranosyl-(1→2)-β-D-glucopyranosyl-(1→3)-[α-L-rhamnopyranosyl-(1→2)]-α-L-arabinopyranoside]	Kudinoside C	–	–	+
46	12-Ursene-3,11,28-triol; (3β,11α)-form, 11-ketone, 3-*O*-[β-D-glucopyranosyl-(1→2)-α-L-arabinopyranosyl-(1→2)-α-L-rhamnopyranoside OR 12-ursene-3,11,28-triol; (3β,11α)-form, 11-ketone, 3-*O*-[β-D-glucopyranosyl-(1→3)-[α-L-arabinopyranosyl-(1→2)]-α-L-rhamnopyranoside OR ursolic acid, 3-*O*-[β-D-glucopyranosyl-(1→2)-α-L-arabinopyranosyl-(1→2)-α-L-rhamnopyranoside] OR ursolic acid, 3-*O*-[β-D-glucopyranosyl-(1→3)-[α-L-arabinopyranosyl-(1→2)]-α-L-rhamnopyranoside]	x	+	+	–
47	3,19-Dihydroxy-24-nor-4(23),12-ursadien-28-oic acid; (3β,19α)-form, 28-*O*-β-D-glucopyranosyl ester	Ilexchinenoside D	+	+	–

Table 2 (*Contd.*)

No.	Chemical name	Synonym	ICL	IAL	IRL
48	3-Hydroxy-12,19-ursadien-28-oic acid; 3β-form, 3-*O*-[β-D-glucopyranosyl-(1→2)-β-D-xylopyranoside], 28-*O*-β-D-glucopyranosyl ester	Ilexsaponin K	−	−	+
49	3,19-Dihydroxy-12-ursen-28-oic acid; (3β,19α)-form, 3-*O*-[β-D-glucopyranosyl-(1→2)-α-L-arabinopyranoside]	Ilexside I	+	−	+
50	3,19-Dihydroxy-12-ursen-28-oic acid; (3β,19α)-form, 3-*O*-[α-L-rhamnopyranosyl-(1→2)-β-D-glucopyranosyl-(1→2)-α-L-arabinopyranoside]	Rotundinoside J	+	−	+
51	3,19-Dihydroxy-12-ursen-28-oic acid; (3β,19α)-form, 3-*O*-β-D-glucuronopyranoside	Ilexasprellanoside C	+	+	+
52	3,19-Dihydroxy-12-ursen-28-oic acid; (3β,19α)-form, 3-*O*-[α-L-arabinopyranosyl-(1→2)-β-D-glucuronopyranoside]	x	−	−	+
53	3,23-Dihydroxy-12,18-ursadien-28-oic acid; (3β,20β)-form, 3-*O*-α-L-arabinopyranoside	x	−	+	+
54	3,19,20-Trihydroxy-12-ursen-28-oic acid; (3β,19α,20β)-form, (28→20)-lactone, 3-*O*-[β-D-glucopyranosyl-(1→2)-β-D-glucopyranosyl-(1→3)-[α-L-rhamnopyranosyl-(1→2)]-α-L-arabinopyranoside]	Ilekudinoside G	−	−	+
55	3,19,20-Trihydroxy-12-ursen-28-oic acid; (3β,19α,20β)-form, (28→20)-lactone, 3-*O*-[β-D-glucopyranosyl-(1→3)-[α-L-rhamnopyranosyl-(1→2)]-α-L-arabinopyranoside]	Ilekudinoside T	−	−	+
56	3,19-Dihydroxy-12-oleanen-28-oic acid; (3β,19α)-form, 3-*O*-β-D-glucuronopyranoside	Ilexasprellanoside F	−	+	−
57	3,19-Dihydroxy-12-ursen-28-oic acid; (3β,19α)-form, 3-*O*-(2-*O*-Acetyl-β-D-xylopyranoside)	Ilexasprellanoside B	+	−	−
58	3-Hydroxy-12,18-ursadien-28-oic acid; (3β,20β)-form, 3-*O*-α-L-arabinopyranoside	x	+	−	+
59	3-Hydroxy-12-ursen-28-oic acid; 3β-form, 3-*O*-[β-D-glucopyranosyl-(1→2)-α-L-arabinopyranoside]	x	+	−	−
60	3-Hydroxy-12,18-ursadien-28-oic acid; 3β-form, 3-*O*-β-D-xylopyranoside	Ilexasprellanoside A	+	+	+
61	3-Hydroxy-12-ursen-28-oic acid; 3β-form, 3-*O*-[β-D-glucopyranosyl-(1→2)-β-D-galactopyranoside]	x	+	−	−
62	3,24-Dihydroxy-12-ursen-28-oic acid; 3β-form, 24-*O*-(4-hydroxy-*E*-cinnamoyl)	Obtusin	−	+	+
63	3,27-Dihydroxy-12-ursen-28-oic acid; 3β-form, 27-*O*-(4-hydroxy-*E*-cinnamoyl)	27-Coumaroyloxyursolic acid	+	+	+

[a] +: appear in the sample, −: not appear in the sample.

Two possible aglycones with similar $[M - H]^-$ ions at *m*/*z* 455.3528 were considered: 12-ursene-3,11,28-triol (3β,11α-isomer, with an 11-ketone group) and ursolic acid. Based on the MS/MS data, compound **46** was tentatively characterized as one of the following isomeric saponins: 12-ursene-3,11,28-triol (3β,11α), 11-ketone, 3-*O*-[β-D-glucopyranosyl-(1→2)-α-L-arabinopyranosyl-(1→2)-α-L-rhamnopyranoside] (**46A**); 12-ursene-3,11,28-triol (3β,11α), 11-ketone, 3-*O*-[β-D-glucopyranosyl-(1→3)-[α-L-arabinopyranosyl-(1→2)]-α-L-rhamnopyranoside] (**46B**); ursolic acid, 3-*O*-[β-D-glucopyranosyl-(1→2)-α-L-arabinopyranosyl-(1→2)-α-L-rhamnopyranoside] (**46C**); or ursolic acid, 3-*O*-[β-D-glucopyranosyl-(1→3)-[α-L-arabinopyranosyl-(1→2)]-α-L-rhamnopyranoside] (**46D**). Compound **46** was identified in both *Ilex cochinchinensis* and *Ilex annamensis*, and all four of these proposed structures have been reported for the first time. The MS/MS spectra of these isomers were highly similar due to subtle differences in glycosidic linkage positions, stereochemistry, and the identical molecular formula of the aglycones, which do not produce distinctive fragment ions. Consequently, the four isomers could not be unambiguously differentiated based on MS/MS data alone.

Tyrosinase inhibitory activity evaluation

The tyrosinase inhibitory activity of leaf extracts from *Ilex annamensis* (IAL), *Ilex cochinchinensis* (ICL), and *Ilex rotunda* (IRL) was evaluated at a concentration of 100 μg mL^{-1}. The results (Table 4) revealed that IAL exhibited the strongest inhibitory effect at 40.70% ± 1.84, followed by ICL at 24.40% ± 1.27, while IRL demonstrated the weakest activity at 14.43% ± 1.53. Although these values are considerably lower than that of the positive control kojic acid (88.36% ± 0.57), they indicate that certain *Ilex* leaf extracts possess moderate natural tyrosinase inhibitory potential. The variation in

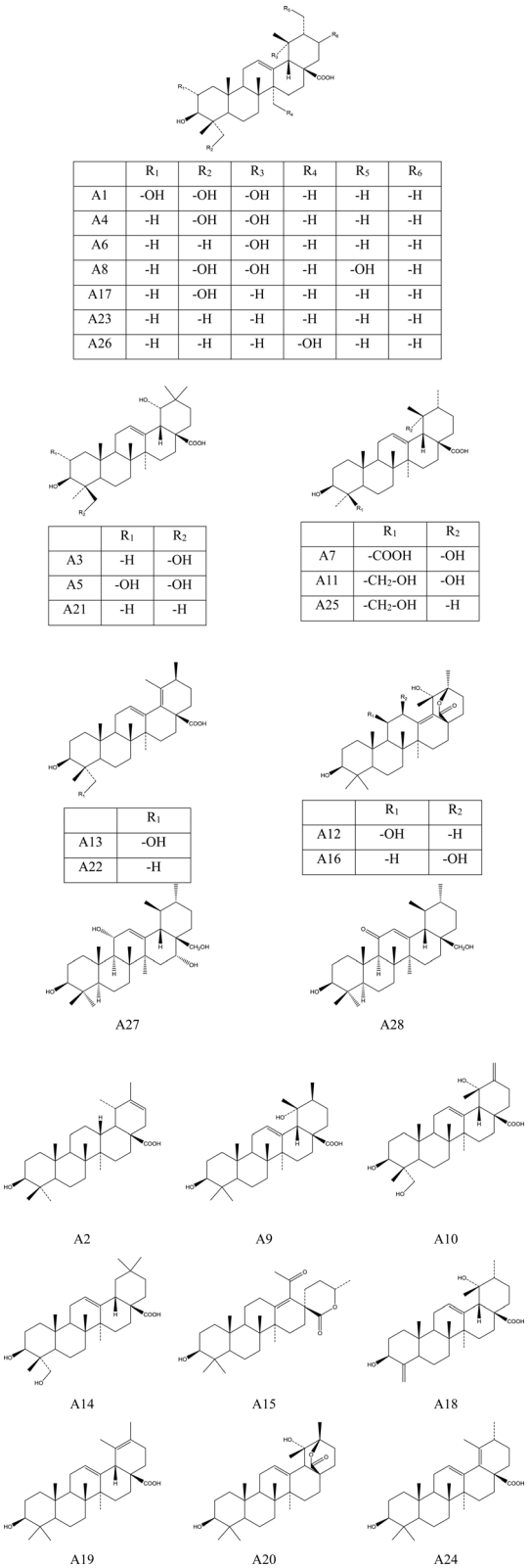

	R_1	R_2	R_3	R_4	R_5	R_6
A1	-OH	-OH	-OH	-H	-H	-H
A4	-H	-OH	-OH	-H	-H	-H
A6	-H	-H	-OH	-H	-H	-H
A8	-H	-OH	-OH	-H	-OH	-H
A17	-H	-OH	-H	-H	-H	-H
A23	-H	-H	-H	-H	-H	-H
A26	-H	-H	-H	-OH	-H	-H

	R_1	R_2
A3	-H	-OH
A5	-OH	-OH
A21	-H	-H

	R_1	R_2
A7	-COOH	-OH
A11	$-CH_2$-OH	-OH
A25	$-CH_2$-OH	-H

	R_1
A13	-OH
A22	-H

	R_1	R_2
A12	-OH	-H
A16	-H	-OH

Fig. 1 Chemical structures of aglycones in *Ilex cochinchinensis*, *Ilex annamensis*, and *Ilex rotunda* leaves.

activity among the three species suggests notable differences in their phytochemical profiles, particularly in bioactive constituents linked to melanogenesis regulation.

Table 3 Structural moieties of identified saponins in *Ilex cochinchinensis*, *Ilex annamensis*, and *Ilex rotunda* leaves

Compound No.	Aglycone	C-3 moiety	C-28/Other moiety
1	**A1**	—	Glc–
2	**A2**	Glc–Xyl–	—
3	**A3**	Glu–	—
4	**A4**	Glc–	Glc–
5	**A4**	Glu–	Glc–
6	**A4**	Glc–	—
7	**A4**	Ara–	Glc–
8	**A5**	—	Glc–
9(A)	**A27**	Glc–Rha–Ara	—
9(B)		Glc-Ara- | Rha	—
10	**A6**	Glu–	Glc–
11	**A7**	—	Glc–
12	**A3**	—	Glc–
13	**A6**	Glc–Ara–	Glc–
14	**A8**	—	Glc–
15	**A27**	Glc–Ara–	—
16	**A9**	Glc–Ara–	—
17	**A10**	—	Glc–
18	**A9**	Rha-Ara- | Glc	Rha–Glc–
19	**A4**	—	Glc–
20	**A9**	Rha–Ara–	Glc–
21	**A6**	Rha–Ara–	Rha–Glc–
22	**A11**	—	Rha–Glc–
23	**A6**	Glc-Glc-Ara- | Rha	—
24	**A12**	Rha-Ara- | Glc	—
25	**A6**	Ara–methyl Glu–	Glc–
26	**A6**	SO_3H–	Glc–
27	**A13**	Glu–	—
28	**A12**	Rha–Glc–	—
29	**A14**	Glu–	Glc–
30	**A4**	Ara–	—
31	**A15**	Rha-Ara- | Glc	—
32	**A11**	—	Glc–
33	**A6**	Ara–	—
34	**A9**	Ara–	Glc–
35	**A16**	Rha–Ara–	—
36	**A4**	Glu–	—
37	**A23**	Glc–Ara–	Glc–
38	**A6**	Ara–Glu–	Glc–
39	**A6**	Rha–Ara–	Glc–
40	**A11**	Glu–	—
41	**A16**	Glc–	—
42	**A16**	Rha–Glc–	—
43	**A16**	Glc-Ara- | Rha	—
44	**A17**	Ara–	Glc–
45	**A16**	Glc-Glc-Ara- | Rha	—
46(A)	**A28**	Glc–Ara–Rha–	—

Table 3 (*Contd.*)

Compound No.	Aglycone	C-3 moiety	C-28/Other moiety
46(B)		Glc-Rha- | Ara	—
46(C)	**A23**	Glc–Ara–Rha–	—
46(D)		Glc-Rha- | Ara	—
47	**A18**	—	Glc–
48	**A19**	Glc–Xyl–	Glc–
49	**A6**	Glc–Ara–	—
50	**A6**	Rha–Glc–Ara–	—
51	**A6**	Glu–	—
52	**A6**	Ara–Glu–	—
53	**A13**	Ara–	—
54	**A20**	Glc-Glc-Ara- | Rha	—
55	**A20**	Glc-Ara- | Rha	—
56	**A21**	Glu–	—
57	**A6**	Acetyl Xyl–	—
58	**A22**	Ara–	—
59	**A23**	Glc–Ara–	—
60	**A24**	Xyl–	—
61	**A23**	Glc–Gal–	—
62	**A25**	—	(C-24) 4-Hydroxy-*E*-cinnamoyl-
63	**A26**	—	(C-27) 4-Hydroxy-*E*-cinnamoyl-

Saponin profiling *via* UHPLC-ESI-QTOF-MS/MS provided insights into these differences. Despite exhibiting the lowest tyrosinase inhibition, IRL contained 34 saponins, but none were novel. ICL, with moderate inhibition, contained 39 saponins, including three previously unreported structures. Interestingly, IAL—which showed the highest inhibitory effect—had 30 saponins, one of which was also found among the three newly identified compounds in ICL. This suggests that not only the number but also the specific structural features of saponins may significantly impact biological activity. The stronger inhibition observed in IAL implies the presence of particularly effective saponins or synergistic interactions with other bioactive compounds not yet fully characterized.

The presence of one novel saponin shared between IAL and ICL might partially explain their higher activities compared to IRL. Moreover, the comparatively lower activity of IRL despite having a similar number of saponins underscores the importance of compound identity and potency over mere quantity. These findings support a positive relationship between the presence of unique or structurally favorable saponins and tyrosinase inhibition. Future work should focus on the targeted isolation and functional validation of these compounds to better understand their mechanisms of action and potential as safer, plant-derived skin-whitening agents.

Experimental

Chemicals and reagents

Deionized water for HPLC; HPLC grade acetonitrile, HPLC grade methanol, analytical grade formic acid (≥98%) were obtained from Scharlau (Barcelona, Spain). L-3,4-dihydroxyphenylalanine (L-DOPA) and kojic acid were purchased from Sigma-Aldrich Pty Ltd. Tyrosinase from mushroom was purchased from BOSF, China. Potassium dihydrogen phosphate (KH_2PO_4) and dimethyl sulfoxide (DMSO) were obtained from Guangdong Guanghua Sci-Tech Co., Ltd.

Sample preparation

Sample collection. *Ilex cochinchinensis*, *Ilex annamensis*, and *Ilex rotunda* leaves were collected from Da Lat City, Lam Dong Province, Vietnam. The botanical identification of specimens was done by Dr. Luong Van Dung from Dalat University, Vietnam. Voucher specimens of *Ilex cochinchinensis* (NaPro0224a),

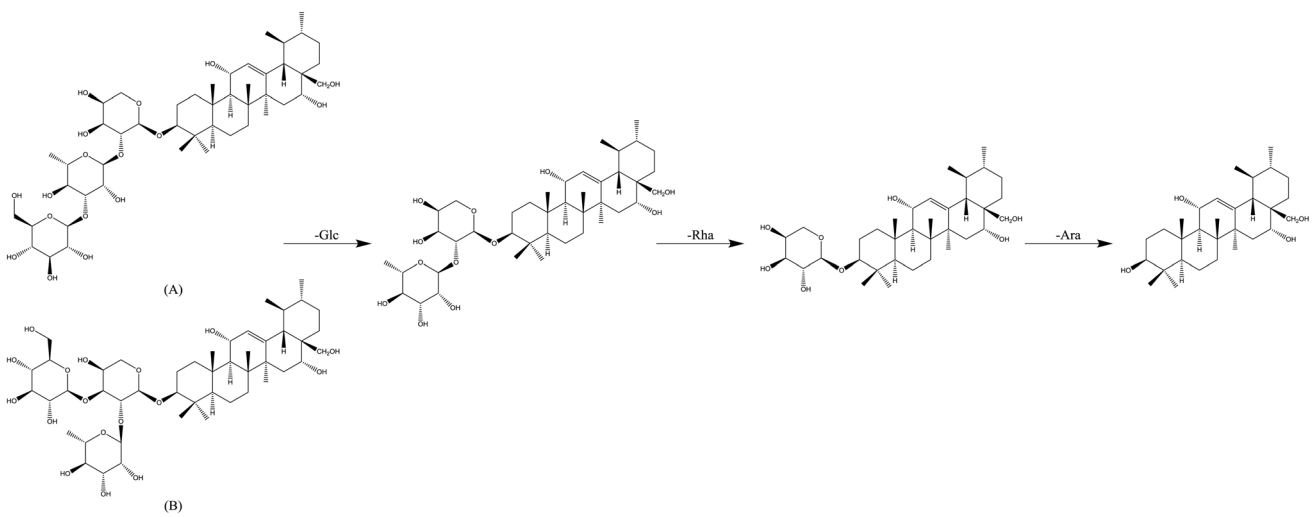

Fig. 2 Fragmentation of two structures of compound **9**.

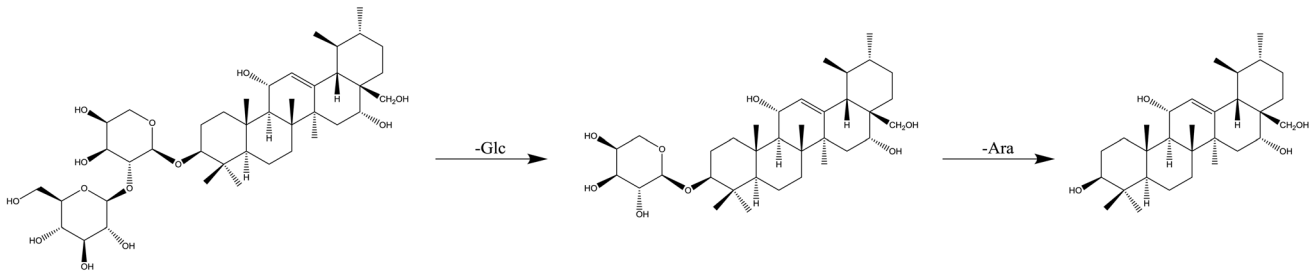

Fig. 3 Fragmentation of compound **15**.

Ilex annamensis (NaPro0224b), and *Ilex rotunda* (NaPro0224c) were deposited in the Institute of Advanced Technology, Vietnam Academy of Science and Technology (VAST). After collection, the fresh samples were cleaned in water to remove sand and soil, left to dry naturally, cut into small pieces, and stored at room temperature until used.

Sample extraction. The leaves of *Ilex cochinchinensis*, *Ilex annamensis*, and *Ilex rotunda* (about 100 g each) were separately subjected to extraction with methanol for 24 hours at room temperature. The extracts were concentrated by removing the solvent using an R-300 Rotary Vacuum Evaporator (BÜCHI, Switzerland). After three times of extraction, the crude extracts were obtained. These samples were prepared at concentration of 200 ppm (in methanol) and 1000 ppm (in DMSO) for UHPLC-QTOF-MS/MS analyses and bioactivity evaluation, respectively.

UHPLC-QTOF-MS/MS analysis

An AB SCIEX X500$_R$ QTOF mass spectrometer (AB SCIEX, USA) connected to an ExionLC™ UHPLC system (AB SCIEX, USA) system by an electrospray ionization (ESI) interface in both negative and positive ion modes, was used for analyses. A Hypersil GOLD C18 column (150 × 2.1 mm, 3 μm) (Thermo

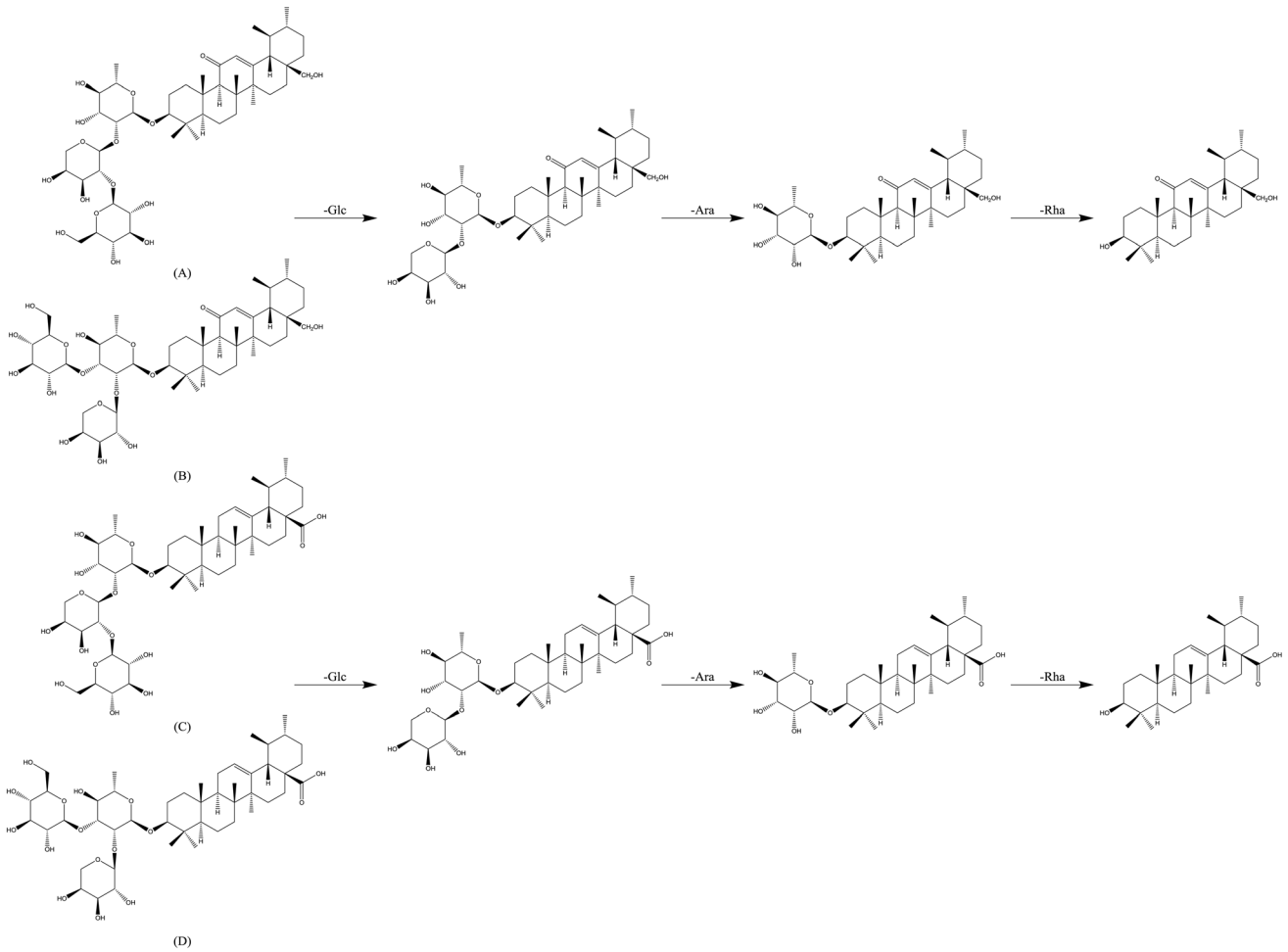

Fig. 4 Fragmentation of four structures of compound **46**.

Table 4 Tyrosinase inhibitory activity of *Ilex cochinchinensis*, *Ilex annamensis*, and *Ilex rotunda* leaves extracts at concentration of 100 (μg mL^{-1})[a]

Sample	Tyrosinase inhibition (%)
Ilex annamensis leaves	40.70 ± 1.84
Ilex cochinchinensis leaves	24.40 ± 1.27
Ilex rotunda leaves	14.43 ± 1.53
Positive control (kojic acid)	88.36 ± 0.57

[a] According to Tukey's HSD test, all samples exhibited statistically significant differences ($p \leq 0.05$).

Fisher Scientific, USA) was used for sample separation at 25 °C. The mobile phase consisted of water containing 0.1% formic acid (A) and acetonitrile containing 0.1% formic acid (B). The elution conditions were as follows: 0–1 min, 2% B; 1–20 min, 2–98% B; 20–25 min, 98% B. The flow rate was 0.4 mL min^{-1}. The sample volume injected was set at 2.0 (μL).

The MS and MS/MS operating parameters were set as follows: the ion source temperature, 500 °C; curtain gas, 30 psi; nebulizer gas (GS 1), 45 psi; heater gas (GS 2), 45 psi. For the negative mode, ion spray voltage was set at −4.5 kV, the declustering potential (DP) was −80 V, the collision energy (CE) was performed at −20 eV, and the collision energy spread (CES) was 10 eV. For the positive mode, ion spray voltage was set at 5.5 kV, the DP was 80 V, the CE was 20 eV, and the CES was 10 eV.

The data were recorded with a SCIEX OS software version 1.2.0.4122 (AB SCIEX, USA).

Tyrosinase inhibitory activity

Tyrosinase inhibitory activity was assayed according to the method described by Wang *et al.* (2014)[31] with some modifications. In summary, 20 μL of the sample was mixed with 40 μL of 50 mM KH_2PO_4 buffer and 80 μL of 150 U per mL enzyme solution. After incubation for 10 minutes at 37 °C, 60 μL of 10 mM L-DOPA was added, and the contents were re-incubated for 20 minutes before measuring the OD values at 475 nm wavelength. Kojic acid used as positive control.

Statistical analyses. The evaluation of tyrosinase inhibitory activity was calculated following the formula below:[32]

$$\%\text{Inhibition} = (\Delta A_{\text{control}} - \Delta A_{\text{sample}})/\Delta A_{\text{control}} \times 100\%$$

where $\Delta A_{\text{control}}$ and ΔA_{sample} were the change of the absorbance without and with the test sample (data was recorded at 475 nm for tyrosinase inhibitory activity).

The data of the bioactivity assays was represented as the means ± standard deviation. One-way ANOVA followed by Tukey's HSD was used to test for differences in mean values between different samples. These tests were performed by Rstudio (version 1.4.1717) software.

Conclusions

This research successfully employed UHPLC-ESI-QTOF-MS/MS to identify and differentiate saponin profiles in the leaf extracts of *Ilex cochinchinensis*, *Ilex annamensis*, and *Ilex rotunda* collected in Vietnam. A total of 63 saponins were tentatively identified, with 39 compounds from *I. cochinchinensis*, 30 from *I. annamensis*, and 34 from *I. rotunda*. Notably, seven saponins were newly reported from *I. cochinchinensis*, including two novel structures corresponding to compound 9 at a retention time (RT) of 11.83 minutes, one novel structure corresponding to compound 15 at RT 12.09 minutes, and four novel structures corresponding to compound 46 at RT 13.71 minutes. Among these, compound 46 was also detected in *I. annamensis*, whereas no new saponins were identified in *I. rotunda*. The distinct chemical profiles enabled clear differentiation among the three species. In addition, tyrosinase inhibitory assays revealed that *I. annamensis* exhibited the highest activity (40.70 ± 1.84%), followed by *I. cochinchinensis* (24.40 ± 1.27%) and *I. rotunda* (14.43 ± 1.53%). Interestingly, the number of identified saponins did not directly correlate with tyrosinase inhibition activity, suggesting that bioactivity may depend more on specific saponin structures rather than total saponin content. These findings contribute valuable insight into the phytochemical diversity and biological potential of *Ilex* species in Vietnam and suggest that *I. annamensis* may serve as a promising natural source for the development of tyrosinase inhibitors in cosmetic and dermatological applications. While the findings are promising, several limitations should be considered, including tentative structural assignments without NMR confirmation, the assessment of tyrosinase inhibition at only a single concentration for comparative screening, and the need for further investigation to clarify the relationship between specific saponin constituents and bioactivity. Future studies should focus on the isolation and structural elucidation of novel saponins using NMR spectroscopy, followed by bioactivity evaluation on pure compounds, in order to confirm new compounds and bioactive candidates through MS-guided approaches.

Author contributions

Pham Hong Ngoc: performed UHPLC-ESI-QTOF-MS/MS analysis, conducted tyrosinase inhibitory assays and statistical analysis, and contributed to manuscript writing. Tran Chieu An: conducted a literature review of previously reported phytochemicals, performed UHPLC-ESI-QTOF-MS/MS analysis, and contributed to manuscript writing. Luong Van Dung: collected plant samples from the field and performed taxonomic identification. Le Tien Dung: co-supervised the research, contributed to manuscript revision and project coordination. Phung Van Trung: supervised the overall project, coordinated all research activities, and critically revised the manuscript.

Conflicts of interest

There are no conflicts to declare.

Data availability

All UHPLC-ESI-QTOF-MS data, including TICs, MS and MS/MS spectra supporting the first report of saponins in this work,

are provided in the supplementary information (SI). Supplementary information: MS and MS/MS data for all detected peaks are summarized in Table 1. See DOI: https://doi.org/10.1039/d5ra05096k.

Acknowledgements

This research was funded by Institute of Advanced Technology – Vietnam Academy of Science and Technology (VAST) under the grant number CSCL19.03/24-25. This research was also supported by Vietnam Academy of Science and Technology (VAST) under grand Excellent Research Group Development Program NCXS02.03/25-26.

Notes and references

1 K. Kothiyal, S. Sudhir, S. C. Sati, S. M. Rawat, M. D. Sati, D. Semwal, B. Semwal, A. Sharma, B. Rawat and A. Kumar, *Nat. Prod. J.*, 2012, **2**(3), 212–224.
2 X. Yao, F. Zhang and R. T. Corlett, *Forests*, 2022, **13**, 94.
3 D. Hao, X. Gu, P. Xiao, Z. Liang, L. Xu and Y. Peng, *Acta Pharm. Sin. B*, 2013, **3**(1), 8–19.
4 S. Y. Kim, M. R. Oh, M. G. Kim, H. J. Chae and S. W. Chae, *BMC Complementary Altern. Med.*, 2015, **15**, 1–8.
5 R. Y. Gan, D. Zhang, M. Wang and H. Corke, *Nutrients*, 2018, **10**(11), 1682.
6 Y. Wu, B. Chai, L. Wang, W. Jiang, M. Hu, Y. Zhao and H. Si, *bioRxiv*, 2018, 457911.
7 S. Jiang, H. Cui, P. Wu, Z. Liu and Z. Zhao, *J. Ethnopharmacol.*, 2019, **245**, 112147.
8 X. Chen, J. Li, R. Yuan, Y. Zhuo, Y. Chen, C. Zhang, M. Chen, H.-W. Gao, Z. Liu, Y. Feng, Z.-T. Wang and S. Yang, *J. Chem.*, 2021, **2021**(1), 9570776.
9 L. Zhang, L. Xu, Y. Ye, M. Zhu, J. Li, Z. Tu, S. Yang and H. Liao, *Ind. Crops Prod.*, 2019, **129**, 156–168.
10 V. Subbiah, B. Zhong, M. A. Nawaz, C. J. Barrow, F. R. Dunshea and H. A. Suleria, *Antioxidants*, 2020, **10**(1), 26.
11 H. Pei, W. Su, M. Gui, M. Dou, Y. Zhang, C. Wang and D. Lu, *Molecules*, 2021, **26**(7), 1855.
12 Y. L. Ji, X. Feng, Y. Q. Chang, Y. G. Zheng, F. J. Hou, D. Zhang and L. Guo, *Arab. J. Chem.*, 2024, **17**(5), 105723.
13 H. N. Pham, C. A. Tran, T. D. Trinh, N. L. N. Thi, H. N. T. Phan, V. N. Le, N. H. Le and V. T. Phung, *J. Anal. Methods Chem.*, 2022, **2022**(1), 1167265.
14 P. H. Ngoc, T. C. An, N. T. Hiep, T. P. H. Nhu, L. N. Hung, N. Q. Trung, Q. M. Bui and V. T. Phung, *J. Anal. Sci. Technol.*, 2023, **14**(1), 14.
15 T. C. An, P. H. Ngoc, N. T. Tuan Hiep, D. D. Long, T. P. H. Nhu and P. V. Trung, *Nat. Prod. Res.*, 2023, **39**(3), 444–452.
16 S. Momtaz, B. M. Mapunya, P. J. Houghton, C. Edgerly, A. Hussein, S. Naidoo and N. Lall, *J. Ethnopharmacol.*, 2008, **119**(3), 507–512.
17 S. Maghsoudi, H. Adibi, M. Hamzeh, M. R. Ashrafi-Kooshk, M. Rezaei-Tavirani and R. Khodarahmi, *J. Rep. Pharm. Sci.*, 2013, **2**(2), 156–164.
18 A. Kilimnik and V. M. Dembitsky, *Mathews J. Pharm. Sci.*, 2016, **1**(1), 1–16.
19 S. Halaouli, M. Asther, K. Kruus, L. Guo, M. Hamdi, J.-C. Sigoillot, M. Asther and A. Lomascolo, *J. Appl. Microbiol.*, 2005, **98**(2), 332–343.
20 R. K. Sahu, A. Roy, J. Dwivedi and A. K. Jha, *Pak. J. Biol. Sci.*, 2014, **17**(1), 146–150.
21 S. Zolghadri, A. Bahrami, M. T. H. Khan, J. Munoz-Munoz, F. Garcia-Molina, F. Garcia-Canovas and A. A. Saboury, *J. Enzyme Inhib. Med. Chem.*, 2019, **34**(1), 279–309.
22 J. Villacís-Chiriboga, A. García-Ruiz, N. Baenas, D. A. Moreno, A. J. Meléndez-Martínez, C. M. Stinco, L. Jerves-Andrade, F. León-Tamariz, J. Ortiz-Ulloa and J. Ruales, *J. Sci. Food Agric.*, 2018, **98**(5), 1927–1934.
23 B. Yang, H. Li, Q. F. Ruan, Y. Y. Xue, D. Cao, X. H. Zhou, S. Q. Jiang, T. Yi, J. Jin and Z. X. Zhao, *J. Pharm. Biomed. Anal.*, 2018, **157**, 44–58.
24 S. J. Yu, Z. P. Yu, Y. Y. Wang, J. Bao, T. Yuan, J. H. Yu and H. Zhang, *J. Asian Nat. Prod. Res.*, 2019, **21**, 316–328.
25 A. Lorini, F. M. Damin, D. N. de Oliveira, R. L. Crizel, H. T. Godoy, V. Galli and A. D. Meinhart, *J. Food Sci.*, 2021, **86**(5), 1599–1619.
26 D. A. Omoboyowa, J. A. Kareem, O. A. Saibu, D. S. Bodun, T. M. Ajayi and O. E. Oyeneyin, *Chem. Afr.*, 2023, **6**(3), 1335–1347.
27 J. Chen, Z. Tao and S. Yang, *Nat. Prod. Res.*, 2025, **39**(12), 3433–3437.
28 L. M. De Souza, N. Dartora, C. T. Scoparo, T. R. Cipriani, P. A. Gorin, M. Iacomini and G. L. Sassaki, Comprehensive analysis of maté (*Ilex paraguariensis*) compounds: development of chemical strategies for matesaponin analysis by mass spectrometry, *J. Chromatogr. A*, 2011, **1218**(41), 7307–7315.
29 M. M. Jin, W. D. Zhang, H. H. Jiang, Y. F. Du, W. Guo, L. Cao and H. J. Xu, UPLC-Q-TOF-MS/MS-guided dereplication of *Pulsatilla chinensis* to identify triterpenoid saponins, *Phytochem. Anal.*, 2018, **29**(5), 516–527.
30 T. C. An, P. H. Ngoc, N. Tuan Hiep, D. D. Long, T. P. H. Nhu and P. V. Trung, Characterisation of saponins from *Hedera nepalensis* in Vietnam northwest mountainous areas with the aid of high-resolution mass spectrometry, *Nat. Prod. Res.*, 2025, **39**(3), 444–452.
31 Y. Wang, M. J. Curtis-Long, B. W. Lee, H. J. Yuk, D. W. Kim, X. F. Tan and K. H. Park, *Bioorg. Med. Chem.*, 2014, **22**(3), 1115–1120.
32 F. Shi, L. Xie, Q. Lin, C. Tong, Q. Fu, J. Xu, J. Xiao and S. Shi, *Food Chem.*, 2020, **312**, 126042.